Impulse penetration into idealized granular beds: Behavior of cumulative surface kinetic energy

Donald P. Visco, Jr. and Saravanan Swaminathan
Department of Chemical Engineering, Box 5013, Tennessee Technological University, Cookeville, Tennessee 38505, USA

T. R. Krishna Mohan,* Adam Sokolow, and Surajit Sen†
Department of Physics, State University of New York, Buffalo, New York 14260-1500, USA
(Received 9 January 2004; revised manuscript received 29 June 2004; published 15 November 2004)

We report a particle dynamics based simulational study of the propagation of δ function mechanical impulses in idealized three-dimensional hexagonal close packed lattices of monosized Hertz spheres. This paper presents five key results on the kinetic energy of grains at the surface of a granular bed after the generation of a normal impulse into the bed. (i) We find that the time integrated or cumulative average kinetic energy per surface grain, κ, drops as an impulse penetrates into the bed. The minimum value of κ, say κ_0, is reached at some time $t=\tau$ after the impulse has been generated. (ii) This value, κ_0, depends upon the restitutional losses at the grain contacts and κ_0 increases as restitutional losses at granular contacts increase in magnitude. (iii) The asymptotic value of κ is denoted by κ_{final}. Our data show that increasing the area across which an impulse is generated, A, leads to $\kappa_{\text{final}} \propto A^{-1/2}$. (iv) If we assign random masses to our monosized grains, κ_{final} grows quadratically as a function of the range of mass variation about a mean mass. We find that at large times, i.e., $t \gg \tau$, $\kappa \propto \{1-\exp[k(1-t/\tau)]\}$, where the constant k is roughly independent of restitution for the typical values of restitution encountered. (v) Our data suggest that at early times, the backscattering process carries signatures of ballistic propagation of the mechanical energy while at late times, the backscattering process is reminiscent of vibrations of an essentially ergodic system. Given the ballisticlike propagation of mechanical energy into granular beds, we conclude that a wave equation based description of mechanical energy propagation into granular beds may not always be appropriate.

DOI: 10.1103/PhysRevE.70.051306 PACS number(s): 81.05.Rm, 83.80.Fg

I. INTRODUCTION

Sound waves of longer wavelength can penetrate deep into soil whereas short wavelengths get rapidly attenuated. It is then natural to argue that sonic probes for detecting and imaging objects buried at shallow depths would fail due to attenuation of short wavelength signals.

Many communities took note when Shukla [1], Sadd [2], Zhu [3], and Rogers and Don [4] studied impulse penetration into shallow granular beds. The two-dimensional (2D) and 3D structures of the beds were studied and details of the impulse generation process were believed to be important parameters that control the nature of energy propagation. Gravitational loading of grains was not believed to be a significant effect in these experimental studies. Rogers and Don [4] successfully discriminated between different shaped objects buried at depths of several centimeters in nominally dry soil using sound bursts. In the same year, House and Pape [5] reported similar findings. The latter authors and others went on to suggest that it might even be possible to image buried objects.

Most early works on acoustic reconnaissance of shallow buried mines are unpublished [6]. Cook and Wormser were the first to publish their work on acoustic detection of nonmetallic land mines [7]. BBN Technologies later reported a study of acoustic mine detection to the US Army [8]. The authors have used transducers to send sinusoidal signals into the bed and have claimed that the frequency range between 100 and 300 Hz works well in detecting small mines at depths of tens of centimeters (cm). Since the early 1990's, Sabatier *et al.* have used continuous sound waves to detect shallow buried antipersonnel landmines that are roughly 10 cm in dimension and typically at depths less than 15 cm [9–12]. McKnight *et al.* [13] have used short duration pulses to detect buried objects and hence the studies in [13] and [4] can be considered to be more closely related to this study. The studies in Refs. [9–13] have used laser-Doppler vibrometry in vegetation-free soil to image shallow buried mines at a forward distance of tens of meters. The continuous wave detection methods are believed to be not as effective at depths in excess of 15 cm and when soil temperatures are below the freezing point.

The above studies suggest something counterintuitive—that sound waves with frequencies of $\sim 10^2$ Hz moving at a velocity of $\sim 10^3$ m/s (at a wavelength of ~ 10 m) can allow imaging of objects that can be as small as $\sim 10^{-2}$ m. Thus one is led to wonder whether a wave equation based analysis of impulse propagation in a granular bed is appropriate. As we shall see, mechanical energy propagation in shallow depths of granular beds, where gravitational loading effects are at best weak compared to the nonlinear Hertz interactions between the grains [14–18], cannot be best described via wave equation based analysis.

Early theoretical and simulational studies by Nesterenko [14–16], Sen *et al.* [17–19], by Coste *et al.* [20], by Hascoet

*On leave from CSIR Centre for Mathematical Modelling and Computer Simulations, Bangalore 560017, India.
†Corresponding author.
Electronic address: sen@dynamics.physics.buffalo.edu

and Herrmann [21], and by Manciu and Sen [22,23] for solving the equations of motion for *individual grains in chains* suggest that granular beds at shallow levels behave very differently than at large depths. Energy propagation is "ballisticlike" at shallow depths and becomes acousticlike as depth increases. Hence wave equation based description of mechanical energy propagation may not be tenable at shallow depths in spite of apparent past successes using such a formulation [24].

Soil grains typically have size distributions ranging between 10^{-4} and 1 mm [25]. The grains are distributed in disordered manner with regions of significant void space and of tight packing. To capture the features of a realistic dry soil bed, it is necessary to construct a large assembly of grains of all sizes and shapes either by deposition [26–28], cluster growth [29–32] or by collective rearrangement models [33–37]. The assembly must be in a local minimum of energy. Although there are several approaches to making such a bed, there appears to be no "silver bullet" to solve this problem.

For the above reasons, in this work, as a first step towards studying mechanical energy propagation in granular beds we address the problem of propagation of impulses in an idealized hexagonal close-packed lattice of elastic spheres. Perhaps controlled experiments with monodisperse quartz beads can be carried out in laboratory environments to explore the validity of our studies. We allow the masses of the grains to vary randomly to get a rough idea of the possible effects of polydispersity. We ignore possible effects associated with loss of grain-grain contacts in our close-packed system by assuming that for large enough system sizes, such effects may not significantly affect our conclusions. The problem of impulse propagation in polydisperse beds, which is significantly more challenging, will build upon the present study, is under way, and will be discussed in future work.

Upon intimate contact, grains repel via the Hertz potential [38]. If δ denotes the overlap between two adjacent spherical grains in contact, where $\delta \equiv d-x$, and where d and x are the distances between the centers of the grains when they barely touch and when they are squeezed together, respectively, the repulsive potential behaves as $V(\delta) \sim \delta^{5/2}$ [38]. Such a potential is steeper than harmonic at large enough compressions but is softer than harmonic at small compressions. This potential, along with the requirement of momentum conservation, leads to effectively ballistic transport of energy [14,39]. The grains do not oscillate against their equilibrium positions, as one would expect on the basis of the wave equation. Instead, they transport the energy and stop, having been slightly displaced from their original positions [40]. Thus the passage of an impulse leaves a region in a compressed state for extended times. Studies of the effects of (terrestrial) gravitational loading on impulse propagation in a chain reveal that gravity does not significantly affect the ballistic propagation behavior at least at length scales $\sim 10^5$ grain diameters [17,40].

Studies [22,41] have established that there is little difference between the propagation of a large area impulse through a perfect close-packed granular bed of monosized spheres and of a single perturbation propagating as a perfect solitary wave through a 1D alignment of grains. The connection between the two becomes exact as the impulse area $A \to \infty$ (see Sen *et al.* in Ref. [22]). Normal impulses generated across finite areas at the surface of a bed result in cone shaped spatial dispersion of propagating energy. In spite of extensive work on simulations on idealized beds [42,43] and by geophysicists on the propagation of *P* and *S* waves [44], much remains to be learned about ways of controlling energy propagation through shallow, disordered granular beds.

II. MODEL AND METHOD

In this work, we consider the propagation of a normal δ-function mechanical impulse imparted onto a fixed area A centered on the bed and the subsequent time dependent behavior of backscattered energy received at the surface of a granular bed. The details of impulse propagation are presented below Eq. (1). We expect that initially, the energy will propagate into the system. The average kinetic energy per grain at the bed surface will hence deplete from a maximum to zero or near zero in this time regime [12,45]. When one grain collides with its neighbor, only a part of the total energy of the grain is transferred to its neighbor. Any energy retained by the first grain results in backscattering. One would expect that the backscattered energy at the surface would initially rapidly increase as backscattering from the first (or subsurface) layer of grains reaches the surface. Subsequent backscattering, which would involve energy transport through multiple granular contacts, would be significantly weaker in magnitude than the initial backscattered energy. Detection of shallow objects, which are likely to produce significant backscattering immediately upon the generation of an impulse, is hence a challenging problem.

We consider the problem of propagation of an impulse in an idealized $40 \times 40 \times 60$ hexagonal-close-packed (hcp) lattice of monodisperse quartz spheres of radius R [12]. We let Y and σ denote the Young's modulus and the Poisson's ratio of quartz. The spheres interact upon compression via the nonlinear Hertz potential [38],

$$V(\delta_{ij}) = a\delta_{ij}^{5/2}, \tag{1}$$

where $a=(2/5D)(R/2)^{1/2}$, $D \equiv (3/2)[(1-\sigma^2)/Y]$ and the grain overlap parameter $\delta_{ij} \equiv 2R-(|\mathbf{r}_i-\mathbf{r}_j|) \geqslant 0$, where (i,j) are neighbors in contact in the hcp lattice.

In our calculations, we set the velocity of all the grains to be zero at $t=0$ except for the grains that sit in an area of size $A=L \times L$ at the bed surface, where L is measured in grain diameters and each grain moves vertically into the bed with velocity $v=v_0$ at $t=0$ (see Fig. 1). Thus we study the propagation of what is effectively a δ-function mechanical impulse into the system. In practice, one can initiate an impulse across a chosen area via some appropriately designed thumper or by irradiation of the bed surface by some appropriate laser beam (see McKnight *et al.* in Ref. [13]). All subsequent grain positions, velocities and accelerations are computed by solving the equation of motion for each grain of mass m_i located at $\mathbf{r}_i$, which reads

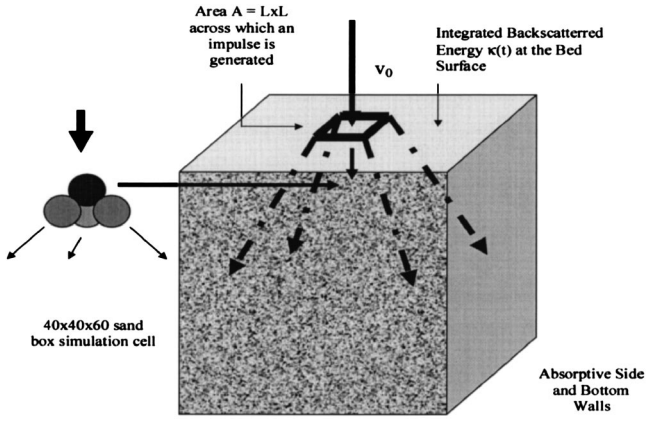

FIG. 1. The figure sketches the propagation of an impulse generated across an area A on a model granular bed. The sketch with three grains on the top left shows how the energy is spread in cone shaped form due to grain coordination.

$$m_i d^2\mathbf{r}_i/dt^2 = \Sigma_{(\text{j neighbors})}\mathbf{F}_{ij}, \tag{2}$$

where the right hand side in Eq. (2) is obtained via Eq. (1). We numerically integrate the coupled equations of motion along x, y, and z coordinates in time via the standard Velocity-Verlet algorithm [14]. The perturbation propagates as a compression pulse into the system. The effect of restitution is included via the intergrain force during loading as follows: F_{load} exceeds that during unloading, F_{unload}. We set

$$F_{\text{unload}}/F_{\text{load}} \equiv 1 - e, \tag{3}$$

where $0<e<1$ defines the restitution parameter. When $e=0$, we get completely elastic behavior and when $e=1$ we get completely inelastic behavior. The effect of positional rearrangements are challenging to incorporate and, to our knowledge, is yet to be attempted by any research group exploring dynamical analyses of granular beds.

We set $R=0.5\times10^{-4}$ m, $\sigma=0.144$, and $Y=7.87\times10^{10}$ Nm^{-2}. Thus $a=1.51\times10^{8}$ Nm$^{-3/2}$ in Eq. (1). The grain mass is set to $m_0=1.41\times10^{-6}$ kg in monodisperse systems. In studies where mass is treated as a random variable, the mean mass is kept as m_0. We use $L=2$, 6, 10, 16, 20, 26, and 30, measured in grain diameters, to explore impulse generation across various areas and restitution values of $e=0$, 0.02, 0.05, 0.1, 0.3, 0.5, 0.7 in our studies. The time step of integration is set at $\Delta t=0.1$ μsec. The impulse propagation speed in this strongly nonlinear system depends upon the details of the initial perturbation. It may be noted that in 1D chains of elastic spheres, the impulse speed $v\sim\xi^{5/4}$, where ξ is the displacement amplitude suffered by the perturbed grain [14–16,19,23]. The impulse propagation speed is typically less than 50 m/s, as would be evident from the data in Fig. 2. This speed is two orders of magnitude slower than the speed of sound in quartz. Impulse propagation in granular media can hence be regarded as a "slow" process involving the travel of a compression pulse. The studies can be typically done on a workstation in several hours of CPU time.

To avoid wall reflection effects in our simulations, the four side walls and the bottom wall are made *energy absorptive*. To insure that the energy incident upon the layer preceding the layer at the wall gets promptly absorbed, we have made the mass of the grains in the wall layer $10^{20}m_0$($m_0=1.41\times10^{-6}$ kg). We also define an energy sink between the grains between the wall layer and the preceding layer by setting $e=1$ between these layers. To insure that we do not introduce any spurious effects, we have checked our results for the time evolution of surface vibrations against a system that is 120 layers deep with an energy sink at layer 120. The results for the 60 and 120 layer systems are indistinguishable. In addition, we insure that a layer of massive grains is placed above the actual surface layer. This layer is introduced to insure that the motion of the surface grains is contained when the backscattered signal reaches the surface grains and sets them to vertical vibration. The abovementioned conditions insure that all the backscattering at the surface of our model bed is backscattering from the elastic spheres in the system and not due to any reflection effects.

III. RESULTS

An impulse, depending upon how it is generated, in general, propagates as a train of solitary waves in a 1D alignment of elastic spheres that are barely in mutual contact [14–23]. When the perturbation is sufficiently weak (typically, a weak perturbation is generated by the impact of a mass, where the impactor is less massive than the masses of the grains in the system) and is a δ function in time, as in

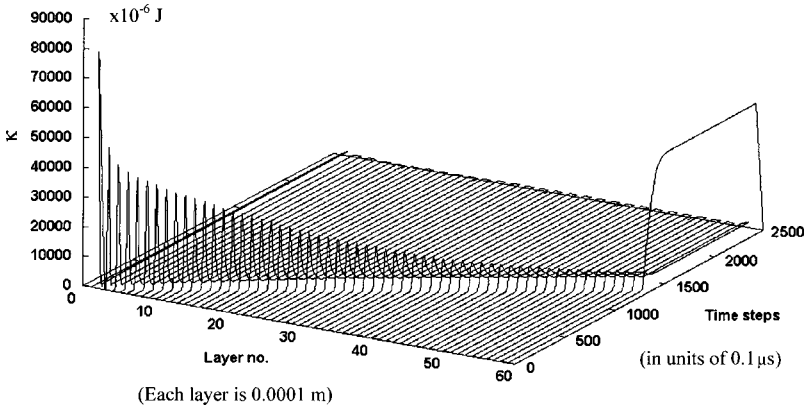

FIG. 2. A 3D plot showing kinetic energy along the Z axis, time steps along the X axis, and layer number along the Y axis. The velocity of the impulse can be read off this plot and turns out to be 50 m/s (see text).

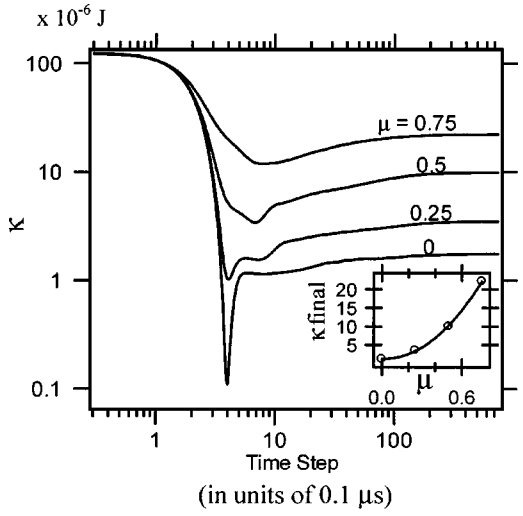

FIG. 3. Behavior of κ vs time shown for beds of monosized spheres where the masses are randomly varied according to Eq. (3). The inset shows that κ_{final} increases quadratically in μ (μ is a dimensionless quantity). The calculations reported are for $A=6$ and $e=0$.

linear response theory, typically, a single, dominant, solitary wave is generated along with one or more solitary waves of amplitudes that are orders of magnitude smaller. We ignore the effects of these tiny secondary solitary waves here. These waves do not add any significant features to the dynamics of the surface grains. A solitary wave is about $6R$ in span. Restitution effects are known to attenuate the amplitude of propagating solitary waves approximately exponentially [46]. We remind the reader that if one considers an infinite 3D granular bed with a close-packed arrangement of grains and generates an impulse across the entire infinite surface of such a system, the problem is effectively a 1D problem [22]. The impulse would hence propagate as a solitary wave.

The impulse propagation behavior, however, is distinct when an impulse is initiated across a small area of the surface. The mechanical energy spreads in a cone shaped form as it propagates into the bed as sketched in Fig. 1. In Fig. 2 we describe data based on large scale particle dynamics based simulations to describe propagation of an impulse into 3D idealized beds as a function of time. We analyze the average cumulative kinetic energy per grain denoted by κ, where

$$\kappa \equiv \Sigma_0^{\mathrm{T}}(1/N_{\mathrm{s}})\Sigma_{\{\text{all surface grains}\}}p_1^2(t)/2m_{\mathrm{i}}, \tag{4}$$

at the surface as a function of time as the system evolves in time from $t=0$ to some maximum time studied, $t=T$ measured in terms of time steps. We denote N_{s} as the number of surface grains. The data in Fig. 2 show that the impulse propagates at a speed of about 50 m/s. The propagation speed depends upon the amplitude of the impulse. However, the numbers are not very different from what is seen in experiments.

In Fig. 3, we present our results for a granular bed of an hcp lattice with monodisperse grains. This data is referred to with a symbol "0" in the figure, where "0" indicates monodispersity. We next present data from dynamical simulations carried out with grains of fixed radius R but with uniform random variation in grain masses described via the formula

$$m_i = m_0[1 + \mu\varepsilon(\mathrm{i})], \tag{5}$$

where μ is set between 0 (which recovers the monodisperse case) and 0.75 (which refers to a high degree of mass variation among the grains in the bed). The quantity $\varepsilon(i)$ varies uniformly randomly with grain position i between -1 and $+1$. We have set μ to fixed values in each polydisperse (again in the restricted sense of mass variation only) bed that we have studied. Figure 3 depicts κ for μ values of 0.25, 0.50, and 0.75, as labeled in Fig. 3. The values $A=6$ and $e=0$ were used in the calculations reported in the lower inset of Fig. 3. In each case study of μ, we find that the average cumulative kinetic energy per surface grain κ reaches a minimum, which we call κ_0, and then grows as a function of time to reach some asymptotic value κ_{final}. The magnitude of κ_{final} increases with increasing μ, i.e., polydispersity leads to enhanced backscattering, which is expected in view of the fact that significant mass contrasts between neighboring grains is expected to give rise to larger backscattering than would be obtained for monodisperse beds. Our simulations are consistent with $\kappa_{\text{final}} \propto \mu^2$ in the range of μ values probed; an observation that reveals that polydispersity can have a marked effect on the magnitude of the backscattered kinetic energy at the bed surface. To our knowledge, experimental data on the effects of polydispersity on enhanced backscattering is currently unavailable.

In Fig. 4 we show the dependence of κ_{final} on the area across which the impulse is generated $A=L\times L$. Our data reveal that $\kappa_{\text{final}} \propto (A^{-1/2})$ or κ_{final}. $L=$const. The larger the L, i.e., the more area consuming the impulse generation process, the less is the energy backscattered to the surface. Thus smaller area impulse generation for less invasive imaging produces higher backscattering and hence makes imaging more challenging. As expected, introducing restitution leads to energy loss at every grain contact and hence further reduces the magnitude of κ_{final}.

Figure 5 shows the same data shown in the main plot of Fig. 3 except that they are in linear scales for specific values of A and e. The data are fitted to a function that grows to saturation as $\kappa \propto (1-\exp[k(1-t/\tau)])$, where τ is the time at which $\kappa \rightarrow \kappa_0$, i.e., as the minimum value of the cumulative kinetic energy per surface grain is reached. From Fig. 5 we find that the constant k in the proposed growth expression for κ is roughly independent of e for $e<0.1$. Figure 5 supports the conclusion that this is a comparative statement as to the value of k based on a 0.1 increment from 0 to 0.1 to 0.5 to 0.6. In the upper inset we find that the value of k has a maximum and has a parabolic behavior with respect to e. When the value of $e \rightarrow 1$, the value of k goes to zero as there is no energy returning to the surface in this limit. The lower inset of Fig. 5 demonstrates the fit to an exponential growth function. We have done many such fits with our data and our

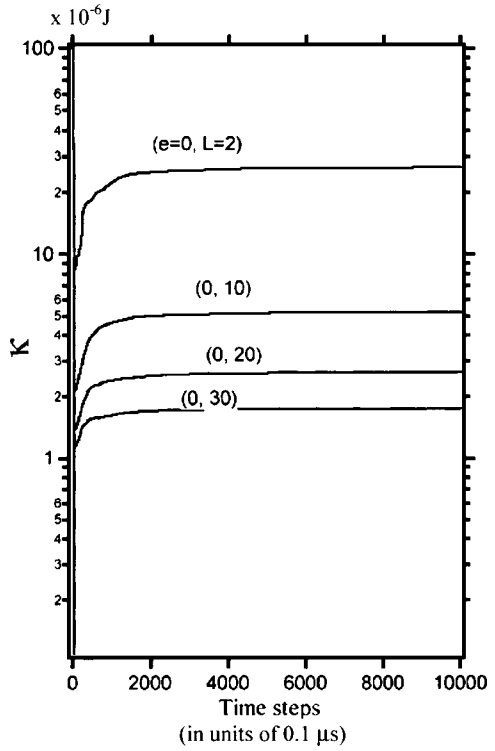

FIG. 4. The plot shows the time evolution of κ as a function of time step (measured in 0.1 μsec) for a monodisperse granular bed. Lower κ values are obtained when impulse area $A=L\times L$ is larger when there is no restitution.

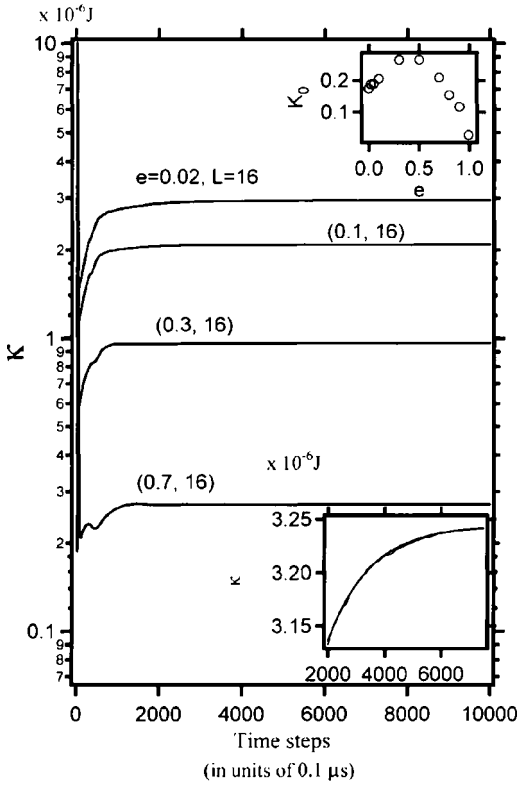

FIG. 5. For a fixed area of $A=16$, the cumulative kinetic energy is plotted vs time steps. This shows that restitution e reduces the magnitude of κ. The upper inset shows that the nature of κ_0, increases as restitution is raised. The lower inset shows that $\kappa \propto \{1-\exp[k(1-t/\tau)]\}$, where $t \gg \tau$, τ being the time at which $\kappa \to \kappa_0$.

calculations suggest that the growth behavior of $\kappa(t)$ shown above holds up well.

IV. ISSUE OF BALLISTIC PROPAGATION

In a recent phenomenological study [45], the nature of backscattering processes have been studied for a 1D layered system in which an energy bundle propagates from one end (the "surface") into the system through the layers. It was assumed that a part p_i of the initial energy is transferred from ith layer to the $(i+1)$th layer, while $(1-p_i)$ is backscattered to the previous layer. One can also introduce restitutional loss in this model by assuming that an amount of energy q_i is lost in each layer. Varying p_i and q_i in arbitrary ways can further enrich the model.

There are two "extreme" ways in which energy transport from one layer to the next can be described in the above-mentioned model. One of these has been called the *exchange case*. In the exchange case, the amount of energy simultaneously propagating in opposite directions through a layer at any given time instant, passes through one another without *any* interaction. *The exchange case mimics a purely ballistic limit of energy propagation through the system*. Table I describes the nature of ballistic propagation for $q_i=0$. Figure 6 reports the cumulative (or time integrated) kinetic energy as a function of time at the surface layer [labeled $\kappa(t)$] in the inset. The main panel shows the instantaneous backscattered energy $e^{\mathrm{bs}}(t)$ as a function of time. It can be clearly seen that in the exchange case, $\kappa(t)$ grows in abrupt jumps rather than as a smooth function. In Fig. 3–5, the growth of $\kappa(t)$ immediately after $\kappa_0(t)$ shows abrupt growth, in a manner characteristic of $\kappa(t)$ for the ballistic propagation case.

TABLE I. Description of energy transmission in a 1D layered system with ballistic energy transport that satisfies the exchange condition (see text in Sec. IV).

Time	$e^{\mathrm{bs}}(t)$	Layer 1	Layer 2	Layer 3	Layer 4	Layer 5
0	0	$1\rightarrow$	0	0	0	0
1	0	$\leftarrow(1-p_1)$	$p_1\rightarrow$	0	0	0
2	$p_1(1-p_1)$	$(1-p_1)^2\rightarrow$	$\leftarrow p_1(1-p_2)$	$p_1p_2\rightarrow$	0	0
3	0	$\leftarrow p_1(1-p_2)$	$(1-p_1)^2\rightarrow$	$\leftarrow p_1p_2(1-p_3)$	$p_1p_2p_3\rightarrow$	0
4	$p_1{}^2(1-p_2)$	$p_1(1-p_1)(1-p_2)\rightarrow$	$\leftarrow p_1p_2(1-p_3)$	$(1-p^1)^2\rightarrow$	$\leftarrow p_1p_2p_3(1-p_4)$	$p_1p_2p_3p_4\rightarrow$

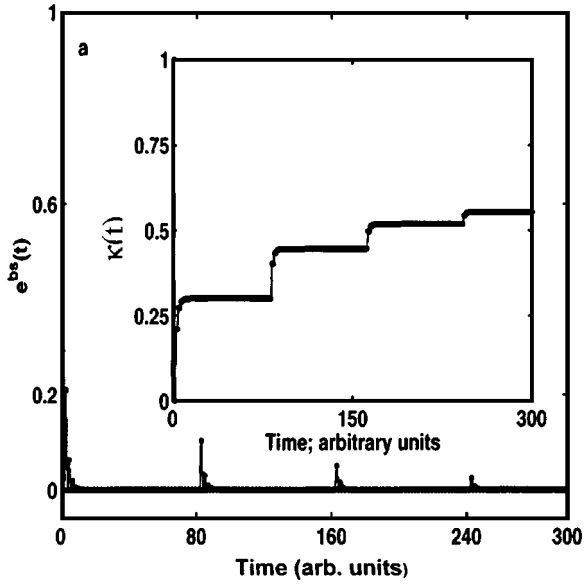

FIG. 6. The backscattered energy at the surface layer of the 1D layer model is shown as a function of time for the exchange model problem (see text). The quantity $e^{bs}(t)$ is the instantaneous backscattered energy. The inset show the step wise growth pattern in the time integrated backscattered energy as a function of time. This quantity is the same as $\kappa(t)$ in our 3D model.

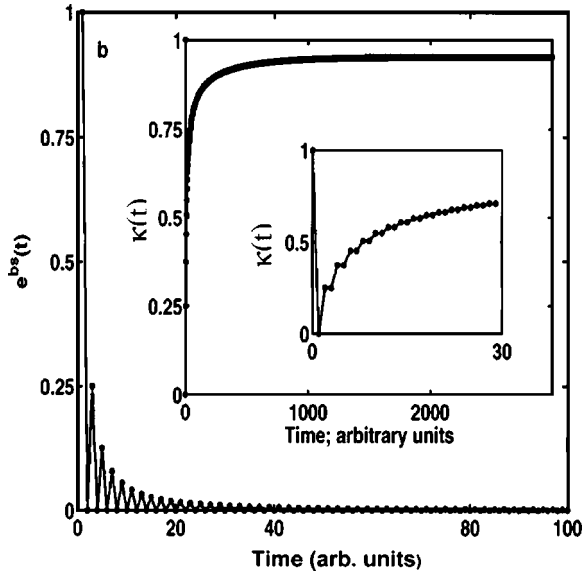

FIG. 7. The backscattered energy at the surface layer of the 1D layer model is shown as a function of time for the equipartition model problem (see text). The quantity $e^{bs}(t)$ is the instantaneous backscattered energy. The insets show the exponentially growing time integrated backscattered energy as a function of time. This quantity is the same as $\kappa(t)$ in our 3D model.

The other extreme case is called the *equipartition case*. In the equipartition case, the simultaneously opposite propagating energy bundles at a given layer at any given time instant is added and halved. The detailed analytic treatment of this model turns out to be a challenge and is worthy of separate consideration [47]. Hence we do not provide detailed analyses of this system. Numerical results to describe backscattering processes for the equipartition case is shown in Fig. 7 [45]. The equipartition case is analogous to an ergodic limit of energy transport through the system. The exponential growth of $\kappa(t)$ in time in the insets of Fig. 7 are distinct from the same in the inset of Fig. 6. The growth pattern in $e^{bs}(t)$ is also distinct in this limit. It may be noted that due to lack of restitutional losses and the one-dimensionality of the model, the magnitude of backscattering is high in our 1D model.

Comparison between the results of our simulational studies reported in Figs. 2–5 and the 1D layer model studies in Figs. 6 and 7 suggest that at short enough times beyond $t=\tau$ when $\kappa=\kappa_0$, the growth of $\kappa(t)$ in time reveals features of ballisticlike propagation whereas the late time exponentiallike growth in $\kappa(t)$ is reminiscent of equipartitionlike behavior of the backscattering process.

Thus we believe that the nonlinear signal propagation in granular beds, which is largely ballisticlike, is dominant at early times in the backscattering process. At late times, there is so much backscattered signal from so many layers that the surface energy can be well approximated via vibrations reminiscent of an ergodic system. Thus the details of system geometry may no longer be strongly relevant to describe the dynamics of the surface grains at late times.

V. SUMMARY AND CONCLUSIONS

We have reported a particle dynamics based simulational study of the propagation of mechanical impulses in idealized hexagonal close packed lattices of monosized Hertz spheres. The walls of the system are kept energy absorptive so as not to produce backscattering. We find that the cumulative average kinetic energy per surface grain, κ, drops as an impulse penetrates into the bed. The minimum value of κ reached, which we call κ_0, depends upon the restitutional losses at the grain contacts and κ_0 increases as e is increased. We denote the time $t=\tau$ as the time at which the minimum value of κ_0 is reached. The asymptotic value of κ is denoted by κ_{final} and our data show that increasing the area across which impulse is generated, A, leads to $\kappa_{\text{final}} \propto A^{-1/2}$. If we assign random masses to our monosized grains, we find that $\kappa_{\text{final}} \propto \mu^2$, where mass variation is denoted by Eq. (3). Finally, we find that for $t \gg \tau$, $\kappa \propto \{1-\exp[k(1-t/\tau)]\}$, where the constant k is roughly independent of e for $e<0.1$. The behavior of κ is consistent with recently reported toy model simulations using an effectively 1D layered system by Krishna Mohan and Sen [45] and with experimental reported in Refs. [12,48]. We believe that the nonlinear propagation characteristics are most important at short times after the generation of the impulse. Details of bed geometry play a crucial role at such early times. The late time behavior of the surface grains is more robust and presumably weakly dependent on the details of the bed itself.

ACKNOWLEDGMENTS

We thank Professor Greg Baker and Samik Sengupta for many discussions. The research has been supported by NSF Grant No. CMS 0070055.

[1] A. Shukla and C. Damania, Exp. Mech. **27**, 268 (1987).
[2] M.H. Sadd, A. Shukla, H. Mei, and C.Y. Zhu, *Micromechanics and Inhomogeneity—The Toshio Mura Anniversary Volume*, edited by G.J. Weng, M. Taya, and H. Abe (Springer, New York, 1989) p. 367.
[3] C.Y. Zhu, A. Shukla, and M.H. Sadd, J. Appl. Mech. **58**, 341 (1991).
[4] A.J. Rogers and C.G. Don, Acoust. Aust. **22**, 5, 1994.
[5] L.J. House and D.B. Pape, U.S. Patent No.5,357,063, 1994.
[6] J.F. Mifsud, Defense Research Laboratory, Univ. of Texas, Report No. DRL-A-95, 1955; S. Rickser, Defense Research Laboratory, University of Texas Report No. DRL-A-98, 1955.
[7] J.C. Cook and J.J. Wormser, IEEE Trans. Geosci. Electron. **GE11**, 135 (1973).
[8] D.A. Sachs, B.G. Watters, P.K. Krumhansel, P.W. Smith, J. Doherty, J. Webb, and A. Davidson, BBN Technical Report No. 7677 (3 volumes), submitted to the U.S. Army Belvoir Research and Development Center, 1992.
[9] J.M. Sabatier, H.E. Bass, L.N. Bolen, K. Attenborough, and V.V.S.S. Sastry, J. Acoust. Soc. Am. **79**, 1345 (1986).
[10] N. Xiang and J.M. Sabatier, Proc. SPIE **4394**, 535 (2001).
[11] D. Donskoy, N. Sedunov, A. Ekimov, and M. Tsionskiy, Proc. SPIE **4394**, 575 (2001).
[12] D. Velea, C. Hickey, and J.M. Sabatier, Proc. SPIE **4394**, 595 (2001).
[13] S.W. McKnight, J. Stott, C.A. DiMarzio, R. Cleveland, and R. Roy, Proc. SPIE **4394**, 627 (2001).
[14] V.F. Nesterenko, J. Appl. Mech. Tech. Phys. **5**, 733 (1983).
[15] V.F. Nesterenko, J. Phys. IV **4**, C8-729 (1994).
[16] V.F. Nesterenko, A.N. Lazaridi, and E.B. Sibiryakov, J. Appl. Mech. Tech. Phys. **36**, 166 (1995).
[17] R.S. Sinkovits and S. Sen, Phys. Rev. Lett. **74**, 2686 (1995).
[18] S. Sen and R.S. Sinkovits, Phys. Rev. E **54**, 6857 (1996).
[19] S. Sen, M. Manciu, and J.D. Wright, Phys. Rev. E **57**, 2386 (1998).
[20] C. Coste, E. Falcon, and S. Fauve, Phys. Rev. E **56**, 6104 (1997).
[21] E. Hascoet, H.J. Herrmann, and V. Loreto, Phys. Rev. E **59**, 3202 (1999).
[22] S. Sen, M. Manciu, V. Tehan, and A.J. Hurd, *The Granular State*, MRS Symposia Proceedings No. 627, edited by S. Sen, and M. Hunt (Materials Research Society, Pittsburgh, 2001); M. Manciu, S. Sen, and A.J. Hurd, *ibid.* p. 3.4.
[23] S. Sen and M. Manciu, Phys. Rev. E **64**, 056605 (2001); M. Manciu, S. Sen, and A.J. Hurd, Physica A **274**, 607 (1999).
[24] G.S. Baker, D.W. Steeples, C. Schmeissner, and K.T. Spikes, Bull. Seismol. Soc. Am. **90**, 494 (2000).
[25] F.E. Richart, Jr., R.D. Woods, and J.R. Hall, Jr., *Vibrations of Soils and Foundations* (Prentice-Hall, Englewood Cliffs, NJ, 1970), and references therein.
[26] E.M. Tory, N.A. Cochrane, and S.R. Waddel, Nature (London) **220**, 1023 (1968); W.M. Visscher and M. Bosterli, *ibid.* **239**, 504 (1972).
[27] E.M. Tory, B.H. Church, M.K. Tam, and M. Ratner, Can. J. Chem. Eng. **51**, 484 (1973).
[28] R. Jullien and P. Meakin, Europhys. Lett. **6**, 629 (1988).
[29] C.H. Bennett, J. Appl. Phys. **43**, 2727 (1972).
[30] A.J. Matheson, J. Phys. C **7**, 2569 (1974).
[31] G.Q. Lu and X. Shi, J. Mater. Sci. Lett. **13**, 1709 (1994).
[32] Y. Konakawa and K. Ishizaki, Powder Technol. **63**, 241 (1990).
[33] J.L. Finney, Mater. Sci. Eng. **23**, 199 (1976).
[34] W.S. Jodrey and E.M. Tory, Powder Technol. **30**, 111 (1981).
[35] W.S. Jodry and E.M. Tory, Phys. Rev. A **32**, 2347 (1985).
[36] G.T. Nolan and P.E. Kavanagh, Powder Technol. **76**, 309 (1993).
[37] A. Yang, G.T. Miller, and L.D. Turcoliver, Phys. Rev. E **53**, 1516 (1996).
[38] H. Hertz, J. Reine Angew. Math. **92**, 156 (1881).
[39] S. Sen and M. Manciu, Phys. Rev. E **64**, 056605 (2001).
[40] M. Manciu, V.N. Tehan, and S. Sen, Chaos **10**, 658 (2000).
[41] M. Manciu, S. Sen, and A.J. Hurd, Physica A **274**, 587 (1999).
[42] S. Sen, M. Manciu, K. Campbell, J. Schein, R.R. Prasad, and M. Krishnan, Proc. SPIE **4394**, 607 (2001).
[43] S. Sen, S. Chakravarti, D.P. Visco, Jr., D.T. Wu, M. Nakagawa, and J.H. Agui, Jr., *Modern Challenges in Statistical Mechanics*, edited by V.M. Kenkre and K. Lindenberg, AIP Conf. Proc. No. 658 (AIP, Melville, NY, 2003), p. 357.
[44] G.S. Baker, C. Schmeissner, D.W. Steeples, and R.G. Plumb, Geophys. Res. Lett. **26**, 279 (1999).
[45] T.R. Krishna Mohan and S. Sen, Phys. Rev. E **67**, 060301(R) (2003).
[46] M. Manciu, S. Sen, and A.J. Hurd, Physica D **157**, 226 (2001).
[47] A. Sokolow and S. Sen (unpublished).
[48] M.J. Naughton, R.S. Shelton, S. Sen, and M. Manciu, in *Proceedings of the 2nd International Conference on the Detection of Abandoned Land Mines—MD'98 Institution of Electrical Engineers Conference Publication No. 458* (IEE, London, 1998), pp. 249–252.